Higher Order Multiphase Image Segmentation and Registration

Stephen Keeling
Institute for Mathematics and Scientific Computing
Karl Franzens University of Graz, Austria

Institute of Mathematics and Image Computing, Universität zu Lübeck

September 28, 2011

Higher Order Models: Total Generalized Variation

Goal: Overcome the essentially piecewise constant model of TV regularization.

Higher Order Models: Total Generalized Variation

Goal: Overcome the essentially piecewise constant model of TV regularization. In the classical approach, minimize:

$$J(I) = \int_\Omega |I - \tilde{I}|^2 + \mathsf{TV}_\alpha(I)$$

Higher Order Models: Total Generalized Variation

Goal: Overcome the essentially piecewise constant model of TV regularization. In the classical approach, minimize:

$$J(I) = \int_\Omega |I - \tilde{I}|^2 + \mathrm{TV}_\alpha(I) \qquad \text{where}$$

$$\alpha \int_\Omega |DI| = \mathrm{TV}_\alpha(I) = \sup \left\{ \int_\Omega I \operatorname{div} \boldsymbol{\psi} : \|\boldsymbol{\psi}\|_\infty \leq \alpha, \boldsymbol{\psi} \in C_0^1(\Omega, \mathbb{R}^n) \right\}$$

Higher Order Models: Total Generalized Variation

Goal: Overcome the essentially piecewise constant model of TV regularization. In the classical approach, minimize:

$$J(I) = \int_\Omega |I - \tilde{I}|^2 + \mathrm{TV}_\alpha(I) \qquad \text{where}$$

$$\alpha \int_\Omega |DI| = \mathrm{TV}_\alpha(I) = \sup \left\{ \int_\Omega I \,\mathrm{div}\, \psi : \|\psi\|_\infty \leq \alpha, \psi \in C_0^1(\Omega, \mathbb{R}^n) \right\}$$

Noisy and TV-reconstructed images:

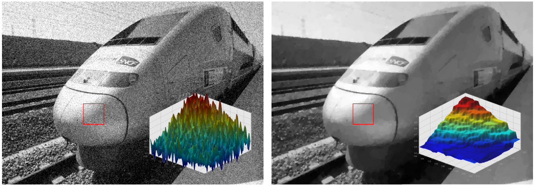

Higher Order Models: Total Generalized Variation

Goal: Develop a functional with a kernel which is richer than piecewise constants.

Higher Order Models: Total Generalized Variation

Goal: Develop a functional with a kernel which is richer than piecewise constants. In the generalized approach, minimize:

$$J(I) = \int_\Omega |I - \tilde{I}|^2 + \mathrm{TGV}_\alpha^k(I)$$

Higher Order Models: Total Generalized Variation

Goal: Develop a functional with a kernel which is richer than piecewise constants. In the generalized approach, minimize:

$$J(I) = \int_\Omega |I - \tilde{I}|^2 + \mathrm{TGV}_{\boldsymbol{\alpha}}^k(I) \qquad \text{where}$$

$$\mathrm{TGV}_{\boldsymbol{\alpha}}^k(I) = \sup\left\{\int_\Omega I \,\mathrm{div}^k \boldsymbol{\psi} : \underbrace{\|\mathrm{div}^l \boldsymbol{\psi}\|_\infty \le \alpha_l}_{l=0,\ldots,k-1}, \boldsymbol{\psi} \in C_0^k(\Omega, \mathrm{Sym}^k(\mathbb{R}^n))\right\}$$

Higher Order Models: Total Generalized Variation

Goal: Develop a functional with a kernel which is richer than piecewise constants. In the generalized approach, minimize:

$$J(I) = \int_\Omega |I - \tilde{I}|^2 + \mathrm{TGV}_{\alpha}^{k}(I) \qquad \text{where}$$

$$\mathrm{TGV}_{\alpha}^{k}(I) = \sup \left\{ \int_\Omega I \,\mathrm{div}^k \psi : \underbrace{\|\mathrm{div}^l \psi\|_\infty \leq \alpha_l}_{l=0,\ldots,k-1}, \psi \in C_0^k(\Omega, \mathrm{Sym}^k(\mathbb{R}^n)) \right\}$$

Noisy and $\mathrm{TGV}_{\alpha}^{2}$-reconstructed images: [Bredies, Kunisch, Pock]

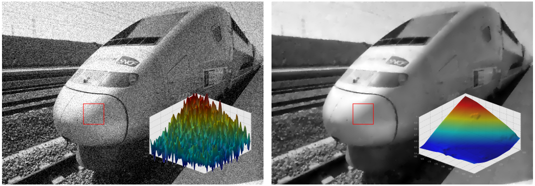

Higher Order Models: Total Generalized Variation

Note: For example, $\mathrm{TGV}_{\alpha}^{2}$ reformulated with duality as

$$\mathrm{TGV}_{\alpha}^{2}(I) = \min_{\boldsymbol{G}} \int_{\Omega} \left\{ \alpha_1 |DI - \boldsymbol{G}| + \frac{1}{2}\alpha_1 |\nabla \boldsymbol{G}^{\mathrm{T}} + \nabla \boldsymbol{G}| \right\}$$

Higher Order Models: Total Generalized Variation

Note: For example, $\mathrm{TGV}_{\boldsymbol{\alpha}}^2$ reformulated with duality as

$$\mathrm{TGV}_{\boldsymbol{\alpha}}^2(I) = \min_{\boldsymbol{G}} \int_\Omega \left\{ \alpha_1 |DI - \boldsymbol{G}| + \tfrac{1}{2}\alpha_1 |\nabla \boldsymbol{G}^{\mathrm{T}} + \nabla \boldsymbol{G}| \right\}$$

Locally:

- DI smooth $\Rightarrow \boldsymbol{G} = \nabla I \approx$ optimal $\Rightarrow \mathrm{TGV}_{\boldsymbol{\alpha}}^2(I) \approx \alpha_0 \int_{\mathrm{loc}} |\nabla^2 I|$.
- I jumps $\Rightarrow \boldsymbol{G} = 0 \approx$ optimal $\Rightarrow \mathrm{TGV}_{\boldsymbol{\alpha}}^2(I) \approx \alpha_1 \int_{\mathrm{loc}} |\nabla I|$.

Higher Order Models: Total Generalized Variation

Note: For example, $\mathrm{TGV}_{\alpha}^{2}$ reformulated with duality as

$$\mathrm{TGV}_{\alpha}^{2}(I) = \min_{\boldsymbol{G}} \int_{\Omega} \left\{ \alpha_1 |DI - \boldsymbol{G}| + \tfrac{1}{2}\alpha_1 |\nabla \boldsymbol{G}^{\mathrm{T}} + \nabla \boldsymbol{G}| \right\}$$

Locally:

- DI smooth $\Rightarrow \boldsymbol{G} = \nabla I \approx$ optimal $\Rightarrow \mathrm{TGV}_{\alpha}^{2}(I) \approx \alpha_0 \int_{\mathrm{loc}} |\nabla^2 I|$.
- I jumps $\Rightarrow \boldsymbol{G} = 0 \approx$ optimal $\Rightarrow \mathrm{TGV}_{\alpha}^{2}(I) \approx \alpha_1 \int_{\mathrm{loc}} |\nabla I|$.

Generally:

- So computing $\mathrm{TGV}_{\alpha}^{2}$ can be seen as solving a minimization problem,
- in which terms of first and second order are optimally balanced out,
- and the vector field $\boldsymbol{G}$ represents the smooth part of the measure DI.

Higer Order Models for Segmentation and Registration

Example: [Video1] [Video2]

Objective: Remove the motion in a DCE-MRI sequence so that individual tissue points can be investigated.

Higer Order Models for Segmentation and Registration

Example: [Video1] [Video2]

Objective: Remove the motion in a DCE-MRI sequence so that individual tissue points can be investigated.

Challenges: Contrast changes with time, and the images are far from piecewise constant.

Higer Order Models for Segmentation and Registration

Example: [Video1] [Video2]

Objective: Remove the motion in a DCE-MRI sequence so that individual tissue points can be investigated.

Challenges: Contrast changes with time, and the images are far from piecewise constant.

Plan: Segment the images, transform the edge sets to diffuse surfaces using blurring, register the diffuse surfaces with progressively less blurring.

Established Approaches to Segmentation

Method of kmeans:

$$\min_{p_k, \chi_k} \left\{ \sum_{k=1}^{K} \int_\Omega |p_k \chi_k - \tilde{I}|^2 : \{p_k\} \in \mathcal{P}^0, \chi_k : \Omega \to \{0, 1\} \right\}$$

Established Approaches to Segmentation

Method of kmeans:

$$\min_{p_k,\chi_k} \left\{ \sum_{k=1}^{K} \int_\Omega |p_k \chi_k - \tilde{I}|^2 : \{p_k\} \in \mathcal{P}^0, \chi_k : \Omega \to \{0,1\} \right\}$$

Minimizing the Mumford-Shah functional:

$$\min_{I,\Gamma} \left\{ \int_\Omega |I - \tilde{I}|^2 + \delta^{-1} \int_{\Omega\setminus\Gamma} |\nabla I|^2 + \beta|\Gamma| \right\}$$

Established Approaches to Segmentation

Method of kmeans:

$$\min_{p_k,\chi_k} \left\{ \sum_{k=1}^{K} \int_\Omega |p_k \chi_k - \tilde{I}|^2 : \{p_k\} \in \mathcal{P}^0, \chi_k : \Omega \to \{0,1\} \right\}$$

Minimizing the Mumford-Shah functional:

$$\min_{I,\Gamma} \left\{ \int_\Omega |I - \tilde{I}|^2 + \delta^{-1} \int_{\Omega \setminus \Gamma} |\nabla I|^2 + \beta |\Gamma| \right\}$$

or the Ambrosio-Tortorelli phase function approximation:

$$\min_{I,\chi} \left\{ \int_\Omega \left[|I - \tilde{I}|^2 + \delta^{-1} |\nabla I|^2 \chi^2 + \epsilon |\nabla \chi|^2 + \epsilon^{-1} |1 - \chi|^2 \right] \right\}$$

Higher Order Counterparts

Method of kmeans:

$$\min_{p_k,\chi_k} \left\{ \sum_{m=1}^{M} \int_\Omega |p_k \chi_k - \tilde{I}|^2 : \{p_k\} \in \mathcal{P}^{m-1}, \chi_k : \Omega \to \{0,1\} \right\}$$

Minimizing the Mumford-Shah functional:

$$\min_{I,\Gamma} \left\{ \int_\Omega |I - \tilde{I}|^2 + \delta^{-1} \int_{\Omega \setminus \Gamma} |\nabla^m I|^2 + \beta |\Gamma| \right\}$$

or the Ambrosio-Tortorelli phase function approximation:

$$\min_{I,\chi} \left\{ \int_\Omega \left[|I - \tilde{I}|^2 + \delta^{-1} |\nabla^m I|^2 \chi^2 + \epsilon |\nabla \chi|^2 + \epsilon^{-1} |1 - \chi|^2 \right] \right\}$$

Representative Problems with These Methods

kmeans leads to staircasing:

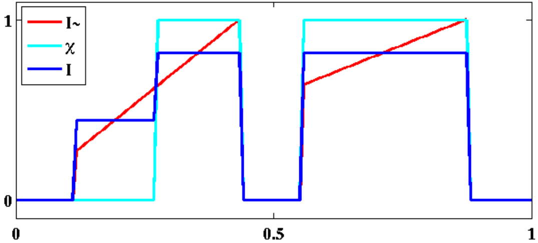

Representative Problems with These Methods

kmeans leads to staircasing:

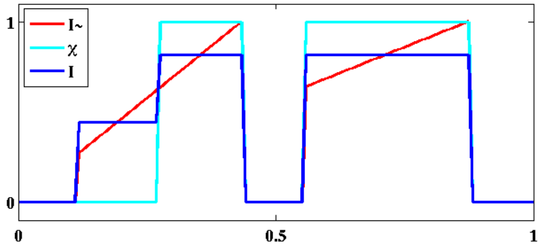

Ambrosio-Tortorelli gives a *fuzzy* edge function:

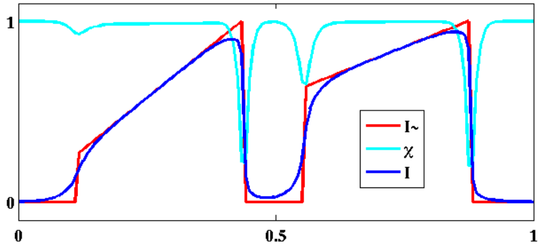

Proposed Multiphase Segmentation Approach

Use multiple phase functions $\{\chi_k\}$ and model functions $\{I_k\}$.

Estimate $\tilde{I} \approx \sum_{k=1}^{K} I_k \chi_k$

Proposed Multiphase Segmentation Approach

Use multiple phase functions $\{\chi_k\}$ and model functions $\{I_k\}$.

Estimate $\tilde{I} \approx \sum_{k=1}^{K} I_k \chi_k$ through minimizing:

$$\min_{\{I_k\},\{\chi_k\}} \left\{ \sum_{k=1}^{K} \int_{\Omega} \left[|I_k - \tilde{I}|^2 {\chi_k}^2 + (\epsilon + \epsilon^{-1} {\chi_k}^2) |\nabla^m I_k|^2 \right. \right.$$

Proposed Multiphase Segmentation Approach

Use multiple phase functions $\{\chi_k\}$ and model functions $\{I_k\}$.

Estimate $\tilde{I} \approx \sum_{k=1}^{K} I_k \chi_k$ through minimizing:

$$\min_{\{I_k\},\{\chi_k\}} \left\{ \sum_{k=1}^{K} \int_\Omega \left[|I_k - \tilde{I}|^2 {\chi_k}^2 + (\epsilon + \epsilon^{-1} {\chi_k}^2) |\nabla^m I_k|^2 \right.\right.$$

$$\left.\left. + \delta |\nabla \chi_k|^2 + \delta^{-1} |\chi_k(\chi_k - 1)|^2 \right] + \delta^{-1} \int_\Omega \left[\sum_{l=1}^{K} \chi_l - 1 \right]^2 \right\}$$

Proposed Multiphase Segmentation Approach

Use multiple phase functions $\{\chi_k\}$ and model functions $\{I_k\}$.

Estimate $\tilde{I} \approx \sum_{k=1}^{K} I_k \chi_k$ through minimizing:

$$\min_{\{I_k\},\{\chi_k\}} \left\{ \sum_{k=1}^{K} \int_\Omega \left[|I_k - \tilde{I}|^2 {\chi_k}^2 + (\epsilon + \epsilon^{-1} {\chi_k}^2) |\nabla^m I_k|^2 \right.\right.$$

$$\left.\left. + \delta |\nabla \chi_k|^2 + \delta^{-1} |\chi_k(\chi_k - 1)|^2 \right] + \delta^{-1} \int_\Omega \left[\sum_{l=1}^{K} \chi_l - 1 \right]^2 \right\}$$

Combines elements of kmeans and Ambrosio Tortorelli.

Proposed Multiphase Segmentation Approach

Simplification to investigate terms:

$$\min_{\{I_k\}} \sum_{k=1}^{K} \int_\Omega \left[|I_k - \tilde{I}|^2 \chi_k + (\epsilon + \epsilon^{-1}\chi_k) |\nabla^m I_k|^2 \right]$$

with each χ_k binary and depending upon $\{I_l\}$:

$$\chi_k(\boldsymbol{x}) = \begin{cases} 1, & |I_k(\boldsymbol{x}) - \tilde{I}(\boldsymbol{x})| < |I_l(\boldsymbol{x}) - \tilde{I}(\boldsymbol{x})|, \quad \forall l \neq k \\ 0, & \text{otherwise.} \end{cases}$$

Proposed Multiphase Segmentation Approach

Simplification to investigate terms:

$$\min_{\{I_k\}} \sum_{k=1}^{K} \int_{\Omega} \left[|I_k - \tilde{I}|^2 \chi_k + (\epsilon + \epsilon^{-1}\chi_k)|\nabla^m I_k|^2 \right]$$

with each χ_k binary and depending upon $\{I_l\}$:

$$\chi_k(\boldsymbol{x}) = \begin{cases} 1, & |I_k(\boldsymbol{x}) - \tilde{I}(\boldsymbol{x})| < |I_l(\boldsymbol{x}) - \tilde{I}(\boldsymbol{x})|, \quad \forall l \neq k \\ 0, & \text{otherwise.} \end{cases}$$

Effects:

- $\epsilon^{-1}\chi_k|\nabla^m I_k|^2 \Rightarrow I_k$ nearly in $\mathcal{P}^{m-1}$ on each connected component of $(\chi_k = 1)$.

Proposed Multiphase Segmentation Approach

Simplification to investigate terms:

$$\min_{\{I_k\}} \sum_{k=1}^{K} \int_\Omega \left[|I_k - \tilde{I}|^2 \chi_k + (\epsilon + \epsilon^{-1}\chi_k) |\nabla^m I_k|^2 \right]$$

with each χ_k binary and depending upon $\{I_l\}$:

$$\chi_k(\boldsymbol{x}) = \begin{cases} 1, & |I_k(\boldsymbol{x}) - \tilde{I}(\boldsymbol{x})| < |I_l(\boldsymbol{x}) - \tilde{I}(\boldsymbol{x})|, \quad \forall l \neq k \\ 0, & \text{otherwise.} \end{cases}$$

Effects:

- $\epsilon^{-1}\chi_k|\nabla^m I_k|^2 \Rightarrow I_k$ nearly in $\mathcal{P}^{m-1}$ on each connected component of $(\chi_k = 1)$.
- $\epsilon|\nabla^m I_k|^2 \Rightarrow I_k$ extended naturally outside $(\chi_k = 1)$.

Proposed Multiphase Segmentation Approach

Simplification to investigate terms:

$$\min_{\{I_k\}} \sum_{k=1}^{K} \int_\Omega \left[|I_k - \tilde{I}|^2 \chi_k + (\epsilon + \epsilon^{-1}\chi_k)|\nabla^m I_k|^2 \right]$$

with each χ_k binary and depending upon $\{I_l\}$:

$$\chi_k(\boldsymbol{x}) = \begin{cases} 1, & |I_k(\boldsymbol{x}) - \tilde{I}(\boldsymbol{x})| < |I_l(\boldsymbol{x}) - \tilde{I}(\boldsymbol{x})|, \quad \forall l \neq k \\ 0, & \text{otherwise.} \end{cases}$$

Effects:

- $\epsilon^{-1}\chi_k|\nabla^m I_k|^2 \Rightarrow I_k$ nearly in $\mathcal{P}^{m-1}$ on each connected component of $(\chi_k = 1)$.
- $\epsilon|\nabla^m I_k|^2 \Rightarrow I_k$ extended naturally outside $(\chi_k = 1)$.
- $|I_k - \tilde{I}|^2\chi_k \Rightarrow I_k \approx \tilde{I}$ on $(\chi_k = 1)$.

Computational Investigation of the Approach

Example: $K = 2$, $m = 2$, $\{\chi_k\}$ & $\{I_k\}$ by splitting, $\chi = \chi_1$.

Given:

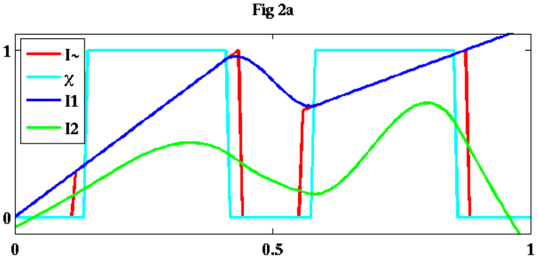

Computational Investigation of the Approach

Example: $K = 2$, $m = 2$, $\{\chi_k\}$ & $\{I_k\}$ by splitting, $\chi = \chi_1$.

Fig 2a

Given:

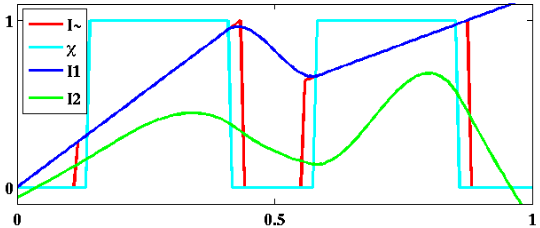

Since $|I_1 - \tilde{I}| < |I_2 - \tilde{I}|$ on and just outside $(\chi = 1)$, next curves:

Fig 2b

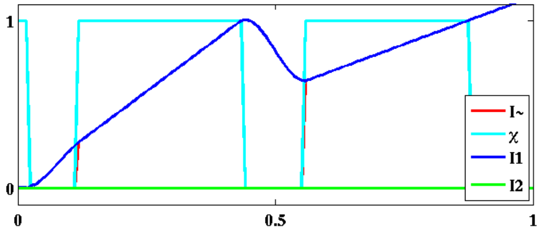

Computational Investigation of the Approach

($\chi = 1$) has grown to include ($\tilde{I} > 0$), but also some ($x < \delta$),

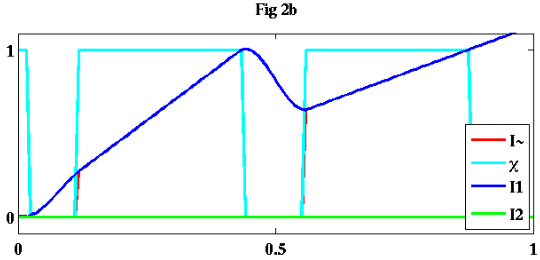

Computational Investigation of the Approach

($\chi = 1$) has grown to include ($\tilde{I} > 0$), but also some ($x < \delta$),

Fig 2b

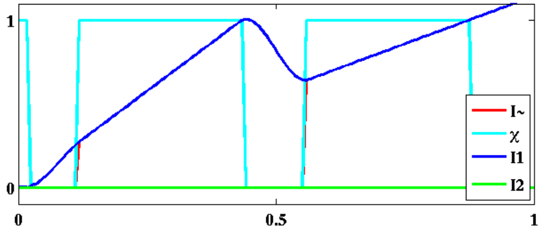

Since $|I_1 - \tilde{I}| < |I_2 - \tilde{I}|$ in ($x < \delta$), converged result:

Fig 2c

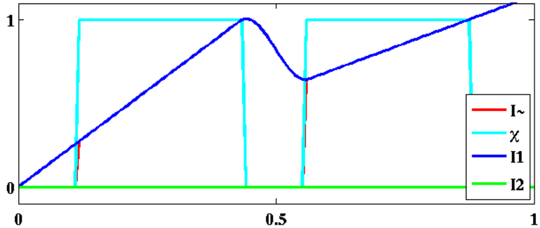

Computational Investigation of the Approach

Converged result:

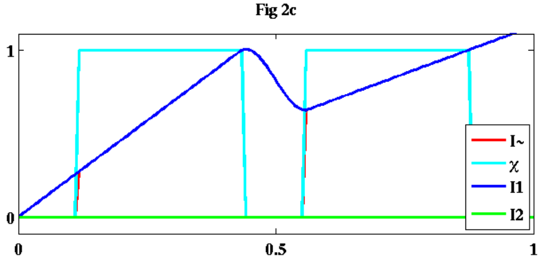

Computational Investigation of the Approach

Converged result:

Fig 2c

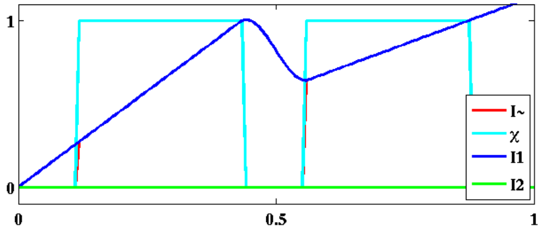

Effects: $(K = 2,\ m = 2,\ \chi = \chi_1)$

- $\epsilon^{-1}\chi_k|\nabla^m I_k|^2 \Rightarrow I_k$ nearly in $\mathcal{P}^{m-1}$ on each connected component of $(\chi_k = 1)$.
- $\epsilon|\nabla^m I_k|^2 \Rightarrow I_k$ extended naturally outside $(\chi_k = 1)$.
- $|I_k - \tilde{I}|^2\chi_k \Rightarrow I_k \approx \tilde{I}$ on $(\chi_k = 1)$.

Computational Investigation of the Approach

Above $\tilde{I}$ was piecewise linear, now piecewise quadratic:

Fig 3a

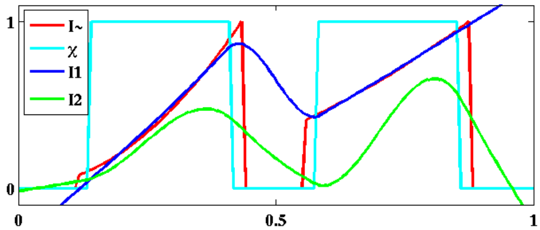

Computational Investigation of the Approach

Above $\tilde{I}$ was piecewise linear, now piecewise quadratic:

Fig 3a

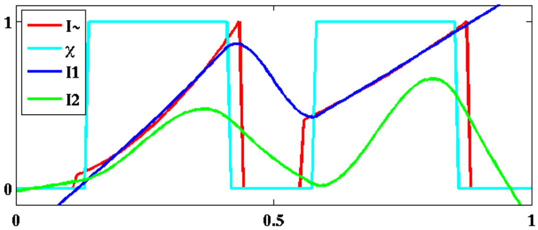

Converged result with an unnatural edge in left piece of ($\tilde{I} > 0$):

Fig 3b

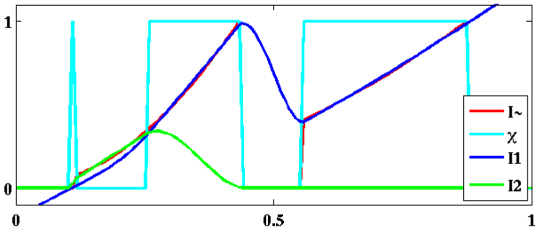

Computational Investigation of the Approach

This result motivates changing $\epsilon^{-1}\chi_k$ to $\alpha\chi_k$ where $\alpha < \epsilon^{-1}$.

New simplified approach:

$$\min_{\{I_k\}} \sum_{k=1}^{K} \int_\Omega \left[|I_k - \tilde{I}|^2 \chi_k + (\epsilon + \alpha\chi_k) |\nabla^m I_k|^2 \right]$$

again with each χ_k binary and depending upon $\{I_l\}$:

$$\chi_k(\boldsymbol{x}) = \begin{cases} 1, & |I_k(\boldsymbol{x}) - \tilde{I}(\boldsymbol{x})| < |I_l(\boldsymbol{x}) - \tilde{I}(\boldsymbol{x})|, \quad \forall l \neq k \\ 0, & \text{otherwise.} \end{cases}$$

Computational Investigation of the Approach

This result motivates changing $\epsilon^{-1}\chi_k$ to $\alpha\chi_k$ where $\alpha < \epsilon^{-1}$.

New simplified approach:

$$\min_{\{I_k\}} \sum_{k=1}^{K} \int_\Omega \left[|I_k - \tilde{I}|^2 \chi_k + (\epsilon + \alpha\chi_k) |\nabla^m I_k|^2 \right]$$

again with each χ_k binary and depending upon $\{I_l\}$:

$$\chi_k(\boldsymbol{x}) = \begin{cases} 1, & |I_k(\boldsymbol{x}) - \tilde{I}(\boldsymbol{x})| < |I_l(\boldsymbol{x}) - \tilde{I}(\boldsymbol{x})|, \quad \forall l \neq k \\ 0, & \text{otherwise.} \end{cases}$$

(Alternative: Increase the order m.)

Computational Investigation of the Approach

$|I_1 - \tilde{I}|$ small near ($\chi = 1$) and $|I_2 - \tilde{I}|$ large near ($\chi = 0$):

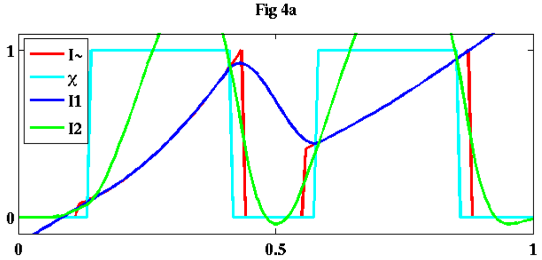

Computational Investigation of the Approach

$|I_1 - \tilde{I}|$ small near ($\chi = 1$) and $|I_2 - \tilde{I}|$ large near ($\chi = 0$):

Fig 4a

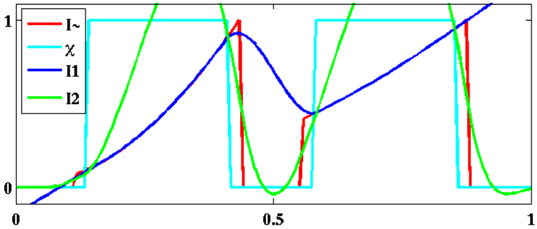

$\alpha < \epsilon^{-1} \Rightarrow |I_1 - \tilde{I}| < |I_2 - \tilde{I}|$ always near ($\chi = 1$). Finally:

Fig 4b

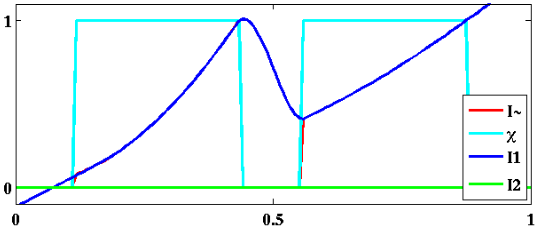

Computational Investigation of the Approach

But the method can still get stuck:

Fig 5

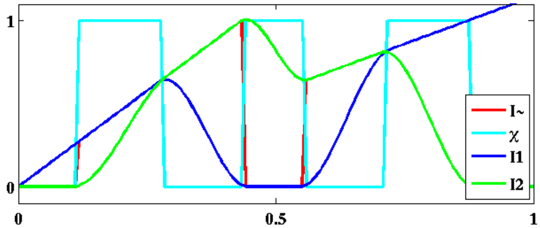

Computational Investigation of the Approach

But the method can still get stuck:

Fig 5

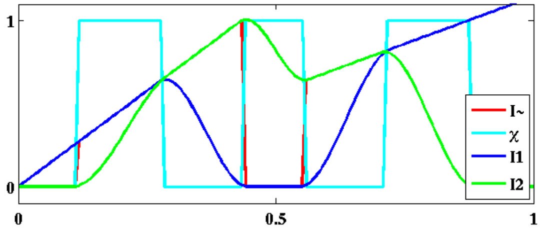

- $\tilde{I}$ is simply piecewise linear.
- $0 \approx |I_1 - \tilde{I}| < |I_2 - \tilde{I}|$ on $(\chi = 1)$.
- $0 \approx |I_2 - \tilde{I}| < |I_1 - \tilde{I}|$ on $(\chi = 0)$.

Computational Investigation of the Approach

But the method can still get stuck:

Fig 5

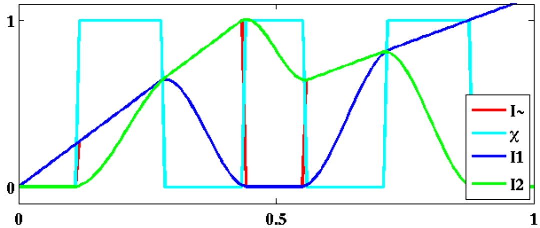

- $\tilde{I}$ is simply piecewise linear.
- $0 \approx |I_1 - \tilde{I}| < |I_2 - \tilde{I}|$ on $(\chi = 1)$.
- $0 \approx |I_2 - \tilde{I}| < |I_1 - \tilde{I}|$ on $(\chi = 0)$.
- Result is converged.

Computational Investigation of the Approach

But the method can still get stuck:

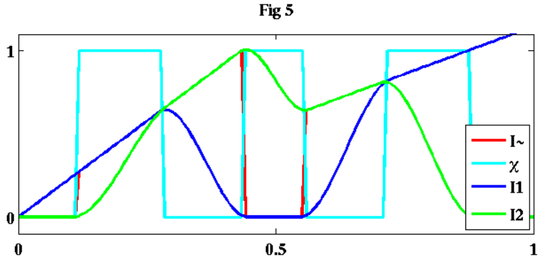

- $\tilde{I}$ is simply piecewise linear.
- $0 \approx |I_1 - \tilde{I}| < |I_2 - \tilde{I}|$ on $(\chi = 1)$.
- $0 \approx |I_2 - \tilde{I}| < |I_1 - \tilde{I}|$ on $(\chi = 0)$.
- Result is converged.
- Such cases are more likely with $K > 2$.

Determining Edges

Examples motivate starting with $\{\chi_k\}$ which respect edges.

Determining Edges

Examples motivate starting with $\{\chi_k\}$ which respect edges.

Determining non-fuzzy edge set $(\chi = 0)$ for $\chi : \Omega \to \{0, 1\}$:

$$\min_{\chi} \int_{\Omega} |I(\chi) - \tilde{I}|^2 \quad \text{where} \quad I(\chi) = \arg\min_{I} \int_{\Omega} \left[|I - \tilde{I}|^2 \chi + (\epsilon + \alpha\chi)|\nabla^m I|^2 \right]$$

Fig 6

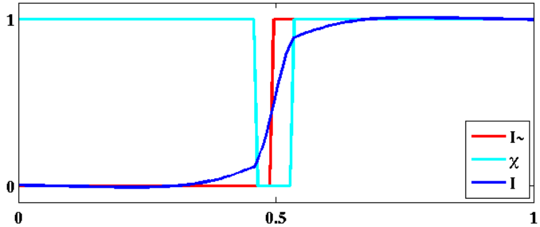

Determining Edges

Examples motivate starting with $\{\chi_k\}$ which respect edges.

Determining non-fuzzy edge set $(\chi = 0)$ for $\chi : \Omega \to \{0, 1\}$:

$$\min_{\chi} \int_\Omega |I(\chi) - \tilde{I}|^2 \quad \text{where} \quad I(\chi) = \arg\min_{I} \int_\Omega \left[|I - \tilde{I}|^2 \chi + (\epsilon + \alpha\chi)|\nabla^m I|^2 \right]$$

Fig 6

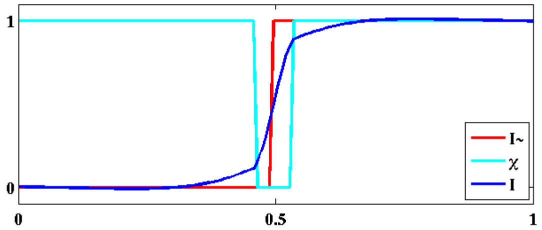

Here the edge set $(\chi = 0) = (|x| < \delta)$ can be determined explicitly by minimizing with respect to δ.

Determining Edges

Examples motivate starting with $\{\chi_k\}$ which respect edges.

Determining non-fuzzy edge set $(\chi = 0)$ for $\chi : \Omega \to \{0, 1\}$:

$$\min_{\chi} \int_{\Omega} |I(\chi) - \tilde{I}|^2 \quad \text{where} \quad I(\chi) = \arg\min_{I} \int_{\Omega} \left[|I - \tilde{I}|^2 \chi + (\epsilon + \alpha\chi) |\nabla^m I|^2 \right]$$

Fig 6

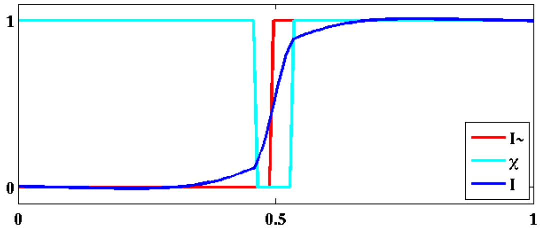

Here the edge set $(\chi = 0) = (|x| < \delta)$ can be determined explicitly by minimizing with respect to δ. In general?...

Edge Determination Approach

Edge set is $(\chi = 0)$ for $\chi : \Omega \to \{0, 1\}$,

$$\chi(\boldsymbol{x}) = \begin{cases} 1, & |I_{\mathrm{b}}(\boldsymbol{x}) - \tilde{E}(\boldsymbol{x})| < |I_{\mathrm{f}}(\boldsymbol{x}) - \tilde{E}(\boldsymbol{x})| \\ 0, & \text{otherwise.} \end{cases}$$

Fuzzy edge function $\tilde{E} = |I_{\mathrm{s}} - \tilde{I}|$,

$$I_{\mathrm{s}} = \arg\min_{I} \int_{\Omega} \left[|I - \tilde{I}|^2 \chi + (\epsilon + \alpha\chi) |\nabla^m I|^2 \right]$$

I_{b} and I_{f} are background and foreground estimations of $\tilde{E}$,

$$I_{\mathrm{b}} = \arg\min_{I} \int_{\Omega} \left[|I - \tilde{E}|^2 \chi + (\epsilon + \alpha\chi) |\nabla I|^2 \right]$$

$$I_{\mathrm{f}} = \arg\min_{I} \int_{\Omega} \left[|I - \tilde{E}|^2 (1 - \chi) + (\epsilon + \alpha(1 - \chi)) |\nabla I|^2 \right]$$

Edge Determination Approach

Example:

Fig 7

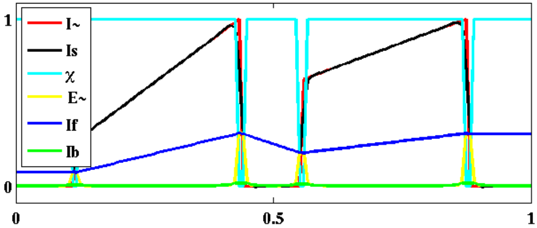

Computed by splitting, starting with $\chi = 1$, then

$$\cdots \to \chi \to I_{\mathrm{s}} \to \tilde{E} \to \{I_{\mathrm{f}}, I_{\mathrm{b}}, \chi\} \to \chi \to \cdots$$

Anisotropic diffusion converges to solution to above system.

Computational Investigation of the Approach

2D Examples:

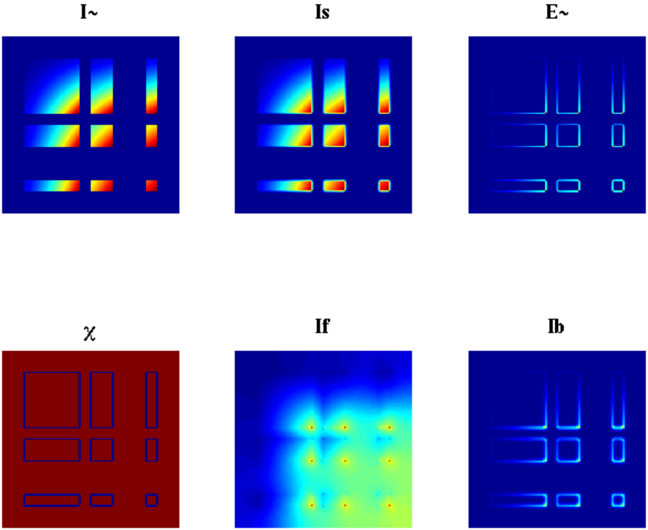

Computational Investigation of the Approach

2D Examples:

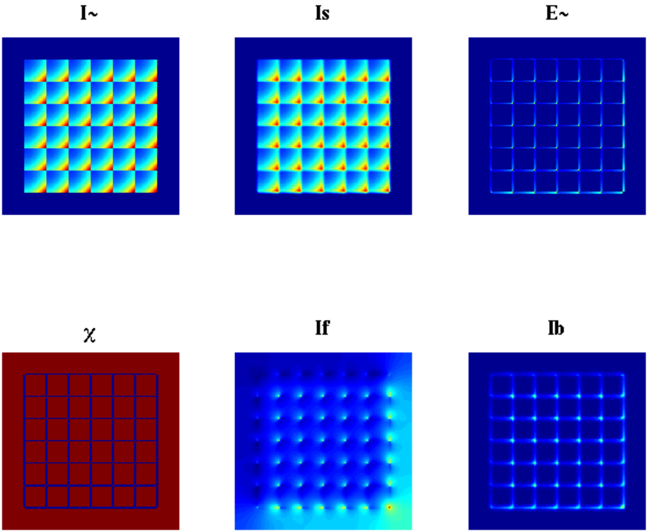

Computational Investigation of the Approach

2D Examples:

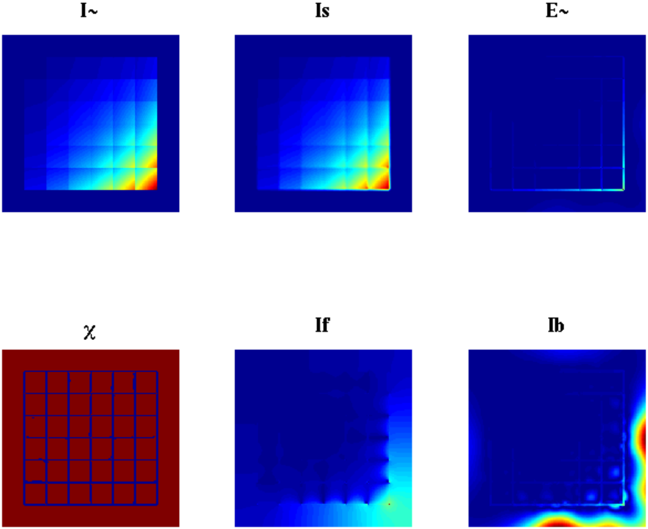

Computational Investigation of the Approach

2D Examples:

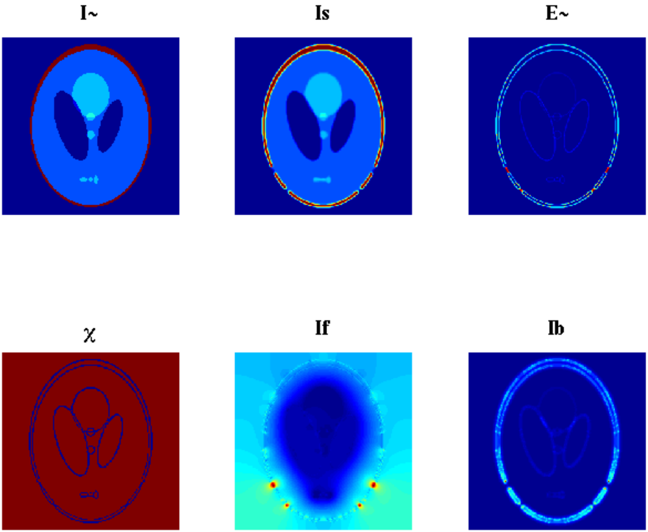

Defining a Segmentation

Define $\sigma = 0, E$ and $\sigma = k, C_k$, where $E = (\chi = 0)$ and $\Omega \backslash E = \cup_k C_k$ and C_k connected. For the above examples:

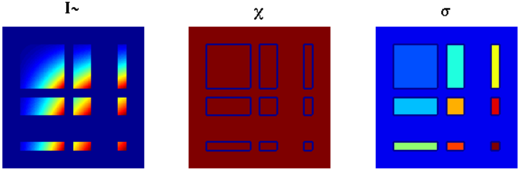

Defining a Segmentation

Define $\sigma = 0, E$ and $\sigma = k, C_k$, where $E = (\chi = 0)$ and $\Omega \backslash E = \cup_k C_k$ and C_k connected. For the above examples:

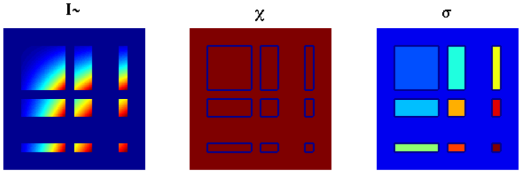

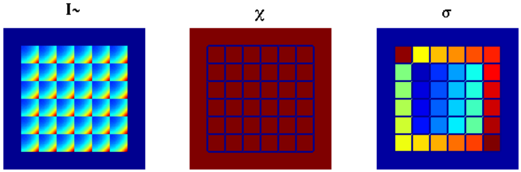

Defining a Segmentation

Define $\sigma = 0, E$ and $\sigma = k, C_k$, where $E = (\chi = 0)$ and $\Omega \backslash E = \cup_k C_k$ and C_k connected. For the above examples:

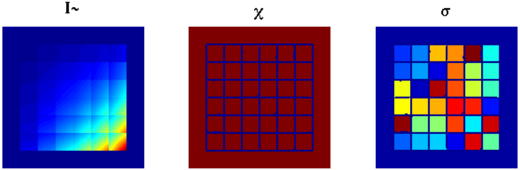

Defining a Segmentation

Define $\sigma = 0, E$ and $\sigma = k, C_k$, where $E = (\chi = 0)$ and $\Omega \backslash E = \cup_k C_k$ and C_k connected. For the above examples:

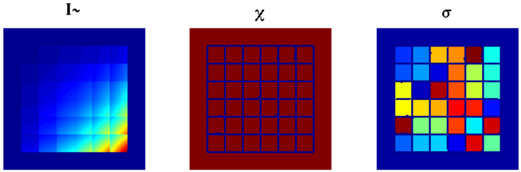

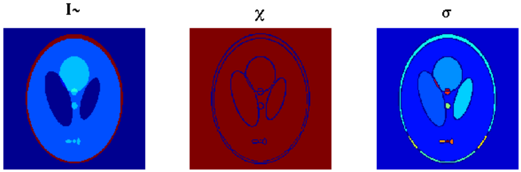

Defining a Segmentation

Assign *orphans* in edge set E to a segment ($\sigma = k$) using best fit to I_k. Store σ and assigned orphans in τ. Define a composite image estimation I_c from updated $\{I_k\}$:

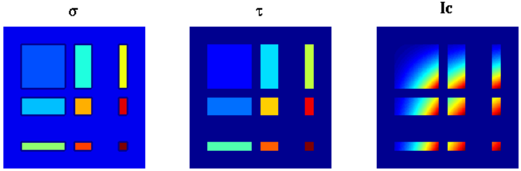

Defining a Segmentation

Assign *orphans* in edge set E to a segment ($\sigma = k$) using best fit to I_k. Store σ and assigned orphans in τ. Define a composite image estimation I_c from updated $\{I_k\}$:

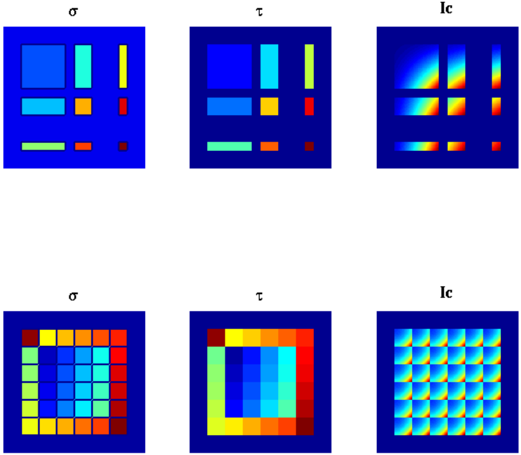

Defining a Segmentation

Assign *orphans* in edge set E to a segment ($\sigma = k$) using best fit to I_k. Store σ and assigned orphans in τ. Define a composite image estimation I_c from updated $\{I_k\}$:

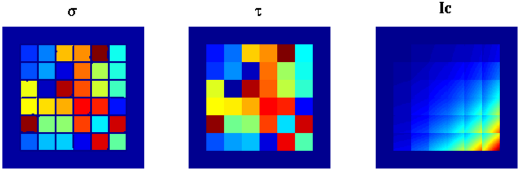

Defining a Segmentation

Assign *orphans* in edge set E to a segment ($\sigma = k$) using best fit to I_k. Store σ and assigned orphans in τ. Define a composite image estimation I_c from updated $\{I_k\}$:

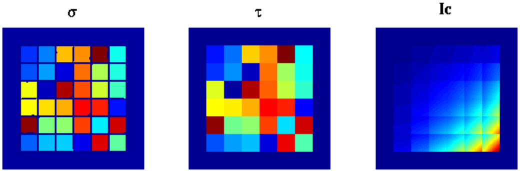

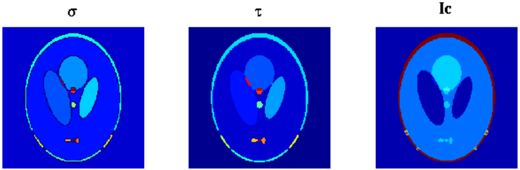

Iterative Refinement of the Segmentation

Refine iteratively with the multiphase segmentation approach to obtain $\{\chi_k\}$ and $\{I_k\}$. Define $I_\mathrm{r} = I_k$ on $(\chi_k = 1)$.

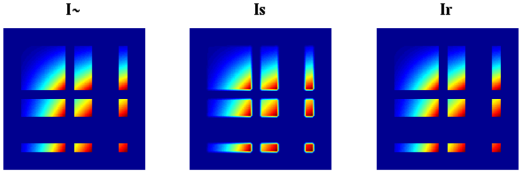

Iterative Refinement of the Segmentation

Refine iteratively with the multiphase segmentation approach to obtain $\{\chi_k\}$ and $\{I_k\}$. Define $I_\mathrm{r} = I_k$ on $(\chi_k = 1)$.

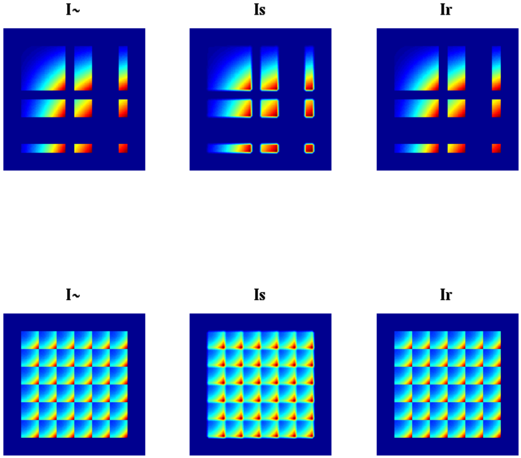

Iterative Refinement of the Segmentation

Refine iteratively with the multiphase segmentation approach to obtain $\{\chi_k\}$ and $\{I_k\}$. Define $I_{\mathrm{r}} = I_k$ on $(\chi_k = 1)$.

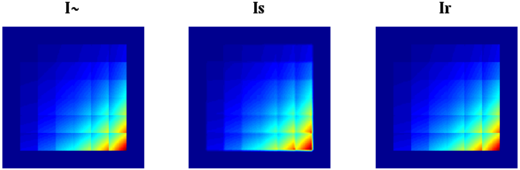

Iterative Refinement of the Segmentation

Refine iteratively with the multiphase segmentation approach to obtain $\{\chi_k\}$ and $\{I_k\}$. Define $I_\mathrm{r} = I_k$ on $(\chi_k = 1)$.

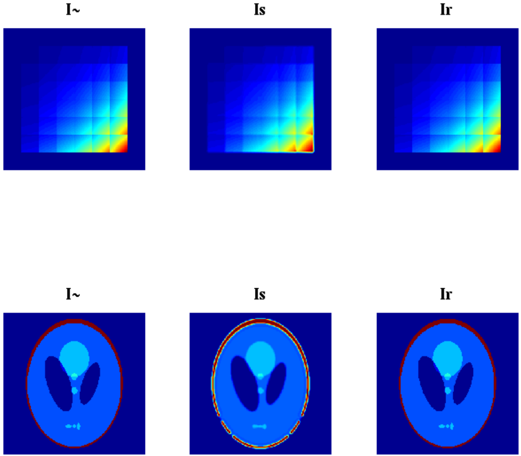

Determining the Number of Phases

Number of connected components (K) can become large!

Determining the Number of Phases

Number of connected components (K) can become large!

Hint from the Four Color Map Theorem?

Determining the Number of Phases

Number of connected components (K) can become large!

Hint from the Four Color Map Theorem?

To reduce number of phase functions, replace τ with

$$\phi(\boldsymbol{x}) = \begin{cases} l, & \chi_{k_i}(\boldsymbol{x}) = 1, \quad i = 1, \ldots, i_l, \quad \partial C_{k_i} \cap \partial C_{k_j} = \emptyset \\ 0, & \text{otherwise} \end{cases} \qquad l = 1, \ldots, L$$

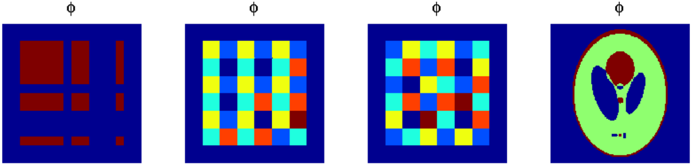

Determining the Number of Phases

Number of connected components (K) can become large!

Hint from the Four Color Map Theorem?

To reduce number of phase functions, replace τ with

$$\phi(\boldsymbol{x}) = \begin{cases} l, & \chi_{k_i}(\boldsymbol{x}) = 1, \quad i = 1, \ldots, i_l, \quad \partial C_{k_i} \cap \partial C_{k_j} = \emptyset \\ 0, & \text{otherwise} \end{cases} \qquad l = 1, \ldots, L$$

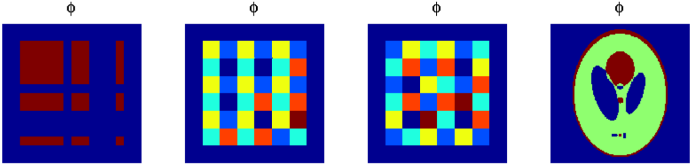

and define

$$\chi_l(\boldsymbol{x}) = \begin{cases} 1, & \phi(\boldsymbol{x}) = l \\ 0, & \text{otherwise} \end{cases} \qquad l = 1, \ldots, L$$

Determining the Number of Phases

Number of connected components (K) can become large!

Hint from the Four Color Map Theorem?

To reduce number of phase functions, replace τ with

$$\phi(\boldsymbol{x}) = \begin{cases} l, & \chi_{k_i}(\boldsymbol{x}) = 1, \quad i = 1, \ldots, i_l, \quad \partial C_{k_i} \cap \partial C_{k_j} = \emptyset \\ 0, & \text{otherwise} \end{cases} \qquad l = 1, \ldots, L$$

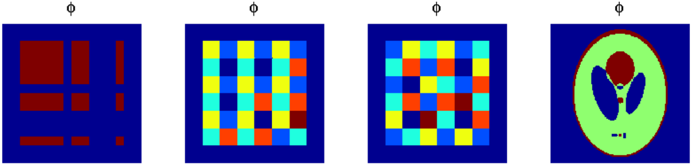

and define

$$\chi_l(\boldsymbol{x}) = \begin{cases} 1, & \phi(\boldsymbol{x}) = l \\ 0, & \text{otherwise} \end{cases} \qquad l = 1, \ldots, L$$

Note: L exceeds 4 in the examples!

Computational Investigation of the Approach

Result for most difficult example ($\tilde{I}$ noisy):

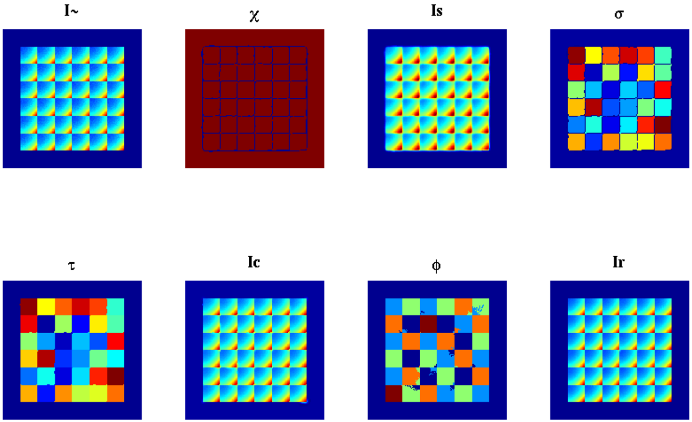

Computational Investigation of the Approach

Result for most difficult example ($\tilde{I}$ noisy):

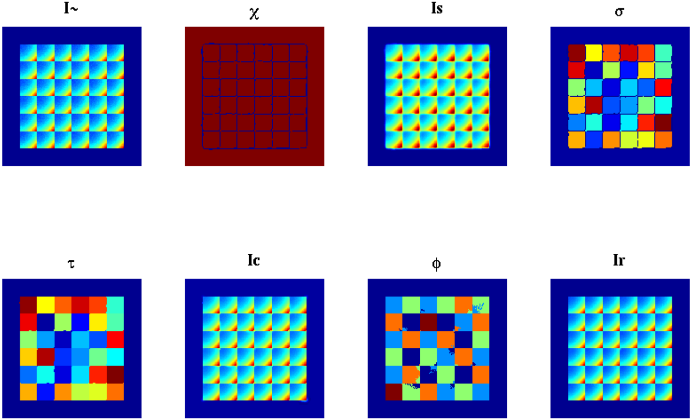

Does $\partial C_{k_i} \cap \partial C_{k_j} = \emptyset$ really hold here?

Computational Investigation of the Approach

Result for most difficult example ($\tilde{I}$ noisy):

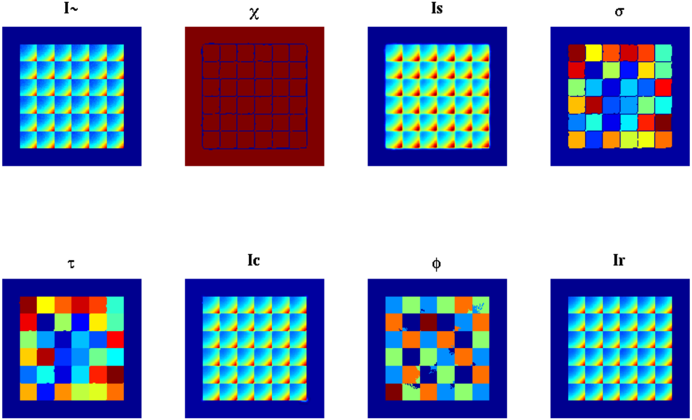

Does $\partial C_{k_i} \cap \partial C_{k_j} = \emptyset$ really hold here?
Yes! Zoom on initial ϕ shows gaps between like-colors cells.

Computational Investigation of the Approach

With sufficient separation between like-colored components:

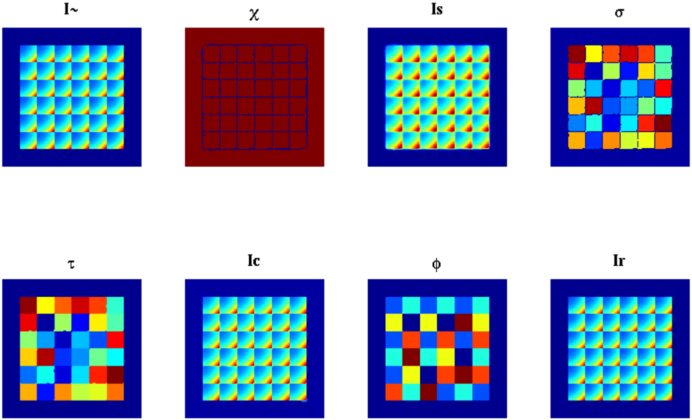

an accurate result is obtained for this challenging example.

Segmentation Regularization

Segments are regularized by smoothing $\{\chi_l\}$ according to

$$\psi_l = \arg\min_{\psi} \int_{\Omega} \left[|\psi - \chi_l|^2 + \delta |\nabla \psi|^2 \right], \quad l = 1, \ldots, L$$

and updating

$$\phi(\boldsymbol{x}) = l, \quad \forall \boldsymbol{x} : \chi_l(\boldsymbol{x}) = 1$$

for redefined

$$\chi_l(\boldsymbol{x}) = \begin{cases} 1, & \psi_l(\boldsymbol{x}) > \psi_k(\boldsymbol{x}), \quad \forall k \neq l \\ 0, & \text{otherwise} \end{cases}$$

Segmentation Regularization

Segments are regularized by smoothing $\{\chi_l\}$ according to

$$\psi_l = \arg\min_{\psi} \int_{\Omega} \left[|\psi - \chi_l|^2 + \delta |\nabla \psi|^2 \right], \quad l = 1, \ldots, L$$

and updating

$$\phi(\boldsymbol{x}) = l, \quad \forall \boldsymbol{x} : \chi_l(\boldsymbol{x}) = 1$$

for redefined

$$\chi_l(\boldsymbol{x}) = \begin{cases} 1, & \psi_l(\boldsymbol{x}) > \psi_k(\boldsymbol{x}), \quad \forall k \neq l \\ 0, & \text{otherwise} \end{cases}$$

Resulting segments are smoother with increasing δ.

Segmentation Regularization

Alternative convex relaxation approach (with Schnörr):

$$\min_{\chi \in C} \left\{ \sum_{l=1}^{L} \int_{\Omega} |I_k - \tilde{I}|^2 \chi_k + \beta TV(\chi_k) \right\}$$

subject to:

$$I_k = \arg\min_{I} \int_{\Omega} \left[|I - \tilde{I}|^2 \chi_k + (\epsilon + \alpha \chi_k) |\nabla^m I|^2 \right]$$

where for $\boldsymbol{\chi} = \{\chi_l\}_{l=1}^{L}$

$$C = \{\boldsymbol{\chi} \in \mathrm{BV}(\Omega, \mathbb{R}^L) : \boldsymbol{\chi}(\boldsymbol{x}) \in \mathcal{S}_L \text{ for a.e. } \boldsymbol{x} \in \Omega\}.$$

and $\mathcal{S}_L$ is the unit simplex in $\mathbb{R}^L$.

Registration of Edge Sets

For mapping a Purkinje fiber network system [Fürtinger]:

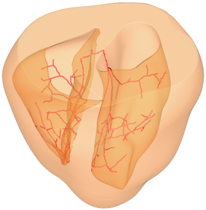

Registration of Edge Sets

For mapping a Purkinje fiber network system [Fürtinger]:

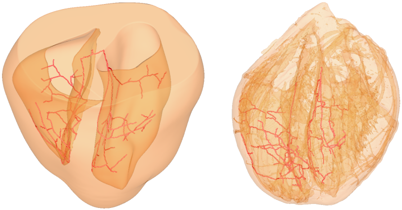

Performed using 2D slices,

$$\min_{\boldsymbol{u}} \int_{\Omega} \left\{ |I_0^{\epsilon} \circ (\mathrm{Id} + \boldsymbol{u}) - I_1^{\epsilon}|^2 + \mu |\nabla \boldsymbol{u}^{\mathrm{T}} + \nabla \boldsymbol{u}|^2 \right\}$$

Registration of Edge Sets

For mapping a Purkinje fiber network system [Fürtinger]:

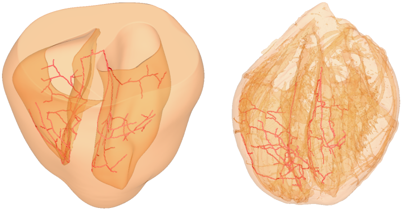

Performed using 2D slices,

$$\min_{\boldsymbol{u}} \int_{\Omega} \left\{ |I_0^{\epsilon} \circ (\mathrm{Id} + \boldsymbol{u}) - I_1^{\epsilon}|^2 + \mu |\nabla \boldsymbol{u}^{\mathrm{T}} + \nabla \boldsymbol{u}|^2 \right\}$$

with diffuse images where registration force strong, then $\epsilon \to 0$.

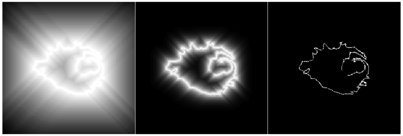

Registration of Edge Sets

But reducing $\epsilon \to 0$
$\Rightarrow$ argmin $= 0$!
Landscape:

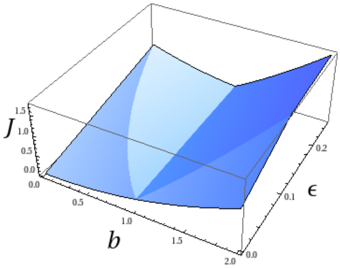

Registration of Edge Sets

But reducing $\epsilon \to 0$
$\Rightarrow$ argmin $= 0$!
Landscape:
(Local convergence)

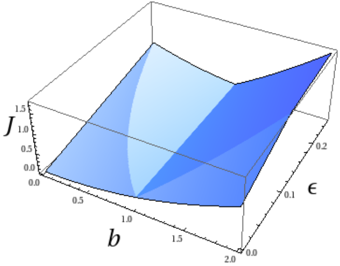

Registration of Edge Sets

But reducing $\epsilon \to 0$
$\Rightarrow$ argmin $= 0$!
Landscape:
(Local convergence)

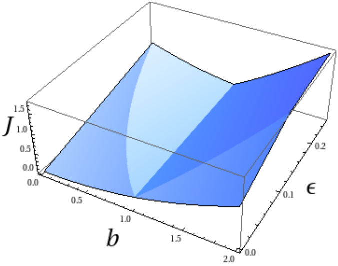

However, with

$$\int_\Omega |I_0^\epsilon \circ (\mathrm{Id} + \boldsymbol{u}) - I_1^\epsilon|^2 \quad \to \quad \int_\Omega |I_0^\epsilon \circ (\mathrm{Id} + \boldsymbol{u}) - I_1^\epsilon|^2 \Big/ \int_\Omega [|I_0^\epsilon|^2 + I_1^\epsilon|^2]$$

the landscape
becomes:

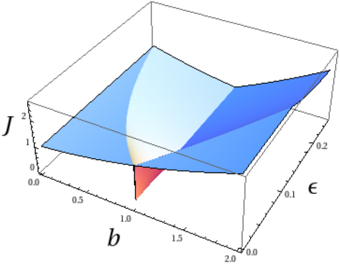

Registration of Edge Sets

But reducing $\epsilon \to 0$
$\Rightarrow$ argmin $= 0$!
Landscape:
(Local convergence)

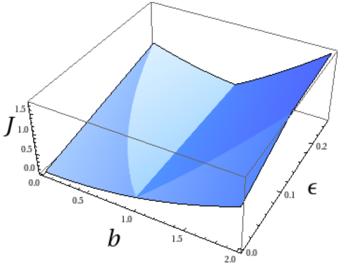

However, with

$$\int_\Omega |I_0^\epsilon \circ (\mathrm{Id} + \boldsymbol{u}) - I_1^\epsilon|^2 \quad \to \quad \int_\Omega |I_0^\epsilon \circ (\mathrm{Id} + \boldsymbol{u}) - I_1^\epsilon|^2 \Big/ \int_\Omega [|I_0^\epsilon|^2 + I_1^\epsilon|^2]$$

the landscape becomes:

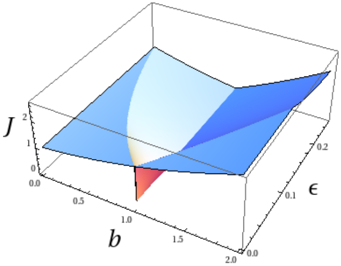

Convergence to Hausdorf distance between edge sets to be shown.

Thank you for your attention!